

# Determination of the Massive Component Contribution from the Analysis of Line Shape Distortions in Diffraction Spectra for Nanocomposite Materials

© O.A. Alekseeva,<sup>1,2</sup> A.A. Nabereznov,<sup>3</sup> Georges-Ivo Ekosse<sup>4</sup>

<sup>1</sup>Peter the Great Saint-Petersburg Polytechnic University,  
195251 St. Petersburg, Russia

<sup>2</sup>Tomsk State University of Control Systems and Radioelectronics,  
634050 Tomsk, Russia

<sup>3</sup>Ioffe Institute,  
194021 St. Petersburg, Russia

<sup>4</sup>University of Venda, University Road,  
0950 Thohoyandou, South Africa  
e-mail: alex.nabereznov@mail.ioffe.ru

Received March 10, 2022

Revised March 10, 2022

Accepted May 17, 2022

Using the analysis of the elastic lines distortions of the diffraction spectra with the involvement of the high order central moments of the distribution, the sensitivity of the developed technique to the presence of an admixture of a bulk component in nanocomposite materials was estimated. Cases for the main types of instrumental resolution functions of diffractometers and functions describing the response from materials embedded in the pore space of nanomatrices such as SBA-15, MCM-41, MCM-48, etc. are considered.

**Keywords:** porous matrices, diffraction, resolution function, nanocomposite materials, elastic peak line shape, higher central moments of distribution.

DOI: 10.21883/TP.2022.09.54692.50-22

## Introduction

Molecular sieves like SBA-15, MCM-41, MCM-48, etc. [1–3] are fine-grained powders with a characteristic granule size of up to several micrometers, and the system of nanometer channels is already implemented at the level of the internal structure each of the granules. Certainly, in the manufacture of nanocomposite materials (NCM) based on molecular sieves, as well as other matrices with nanometer-scale channels (pores) (porous glasses, artificial opals, chrysotile asbestos, etc. [4,5]), the question often arises about the quality of the obtained NCM: first of all, about the possible admixture of bulk material. Indeed, when the pore space of the matrices is filled with the introduced material, especially when it is introduced from an aqueous solution, the probability of the appearance of the contribution of the bulk component is not small, since it can appear due to crystallization not in the pores, but in the free space between the grains of molecular sieves or in large-scale defects of the matrices themselves in the case of porous glasses, opals and chrysotile asbestos. Such an impurity can significantly change the properties of nanocomposites as a whole; therefore, already at the stage of preparing nanocomposites, it is desirable to be able to estimate the contribution of the bulk component. In addition, nanocomposites may also contain impurities of the amorphous phase [6,7], which is rather difficult to

distinguish in diffraction spectra due to the presence of a large background from the nanoporous matrix itself. Thus, conducting a preliminary analysis of the quality of a sample even at the stage of its manufacture and/or refinement of the manufacturing technology becomes very important, and it is desirable to carry out this procedure rather quickly. From this point of view, X-ray or neutron diffraction is one of the most accessible and informative methods for conducting such a preliminary analysis of the NCM structure. In the previous paper [8], we considered distortions of the elastic peak line shape for a mixture of bulk and nanostructured fractions in cases where the instrumental resolution of the diffractometer and the NCM response were described by the same functions (Gaussian, Lorentzian or Voigtian), by analyzing the changes in dispersion, asymmetries, and kurtosis [9] observed at different ratios of fractions and for different characteristic sizes of nanoparticles embedded in the pore space of matrices. The purpose of this paper was to consider cross variants, i.e., cases where the functions for describing the profiles of elastic reflections for the bulk and nanostructured phases differ.

## 1. Initial conditions

The main initial formulas used in the calculations and the starting parameters are given in the article [8], so here we only recall the main provisions and the essence

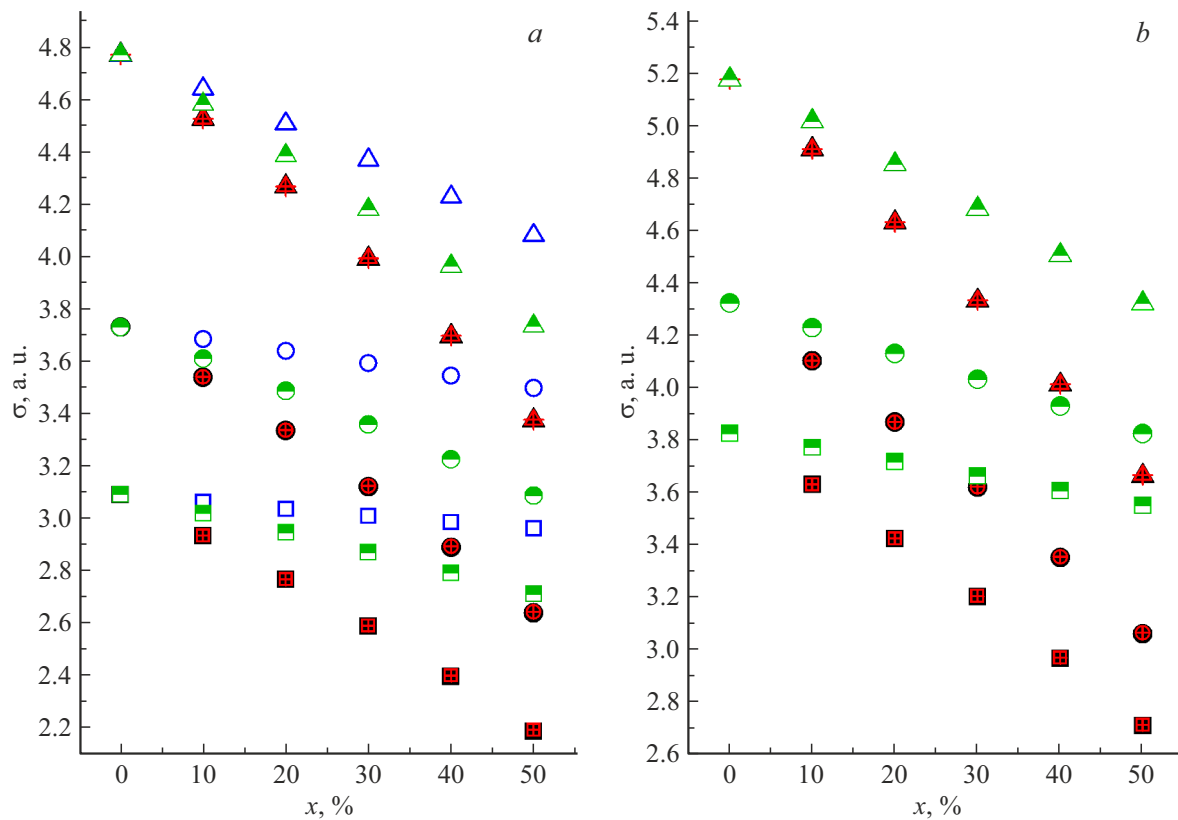


**Figure 1.** The change in the dispersion ( $\sigma$ ) for the Bragg reflection with an increase in the percentage of the bulk material phase in the sample ( $x$ ) in the case of various combinations of nanophase and bulk line shapes: the nanostructured phase is described either by a pseudo-Voigtian (*a*) or Lorentzian (*b*); the bulk one — by Gaussian (black filled symbols), squared Lorentzian (red symbols (in online version)). The half-filled green symbols (in the online version) in both cases correspond to the case of the same line shape. Squares correspond to particle size 80 nm, circles — 40 nm, triangles — 20 nm.

of the approach used in the simulation. In this paper, as we used, as in [8], the setup parameters of a FIRE-POD E9 high resolution neutron diffractometer (Helmholtz Zentrum Berlin, Germany). When describing the experimentally observed shape of the elastic reflection line and instrumental resolution, the following functions were used: Gaussian (1), Lorentzian (2), squared Lorentzian (3) and pseudo-Voigtian (4):

$$G(x) = \frac{2}{H} \sqrt{\frac{\ln 2}{\pi}} \exp\left(-\frac{H}{2} \sqrt{\frac{\pi}{\ln 2}} x^2\right), \quad (1)$$

$$L(x) = \frac{2}{\pi H \left(1 + \frac{4}{H^2} x^2\right)}, \quad (2)$$

$$SqL(x) = \frac{4\sqrt{\sqrt{2}-1}}{\pi H \left(1 + \frac{4(\sqrt{2}-1)}{H^2} x^2\right)^2}, \quad (3)$$

$$pV(x) = pV(x) = \eta L(x) + (1 - \eta)G(x). \quad (4)$$

Here, in all functions, the parameter  $H$  is the width of the elastic peak at half maximum. The parameter  $0 \leq \eta \leq 1$  in formula (4) corresponds to the relative contribution of the Lorentzian. All the above functions are normalized to one.

The following combinations of functions describing the contribution of the mass and nanostructured fractions were analyzed:

- 1) the nanostructured phase is described by the pseudo-Voigtian (4), while the bulk fraction is described either by the Gaussian (1), or by the Lorentzian (2), or by the squared Lorentzian (3);
- 2) the nanostructured phase is described by the Lorentzian (2), while the bulk fraction is described either by the Gaussian (1) or by the squared Lorentzian (3);
- 3) the nanostructured phase is described by a squared Lorentzian (3), while the bulk material admixture is described by a Gaussian (1).

In the case of a bulk fraction, the parameter  $H$  was taken equal to the width of the instrumental resolution function calculated by the Cagliotti formula [10]:

$$H_{instr}^2 = U \operatorname{tg}^2 \theta + V \operatorname{tg} \theta + W. \quad (5)$$

Here, the parameters  $U, V, W$  were taken for the instrumental resolution function of a FIREPOD E9 high-resolution neutron diffractometer (Helmholtz Zentrum Berlin, Germany).

For the nanostructured phase, the parameter  $H$  was calculated as the total contribution from the instrumental

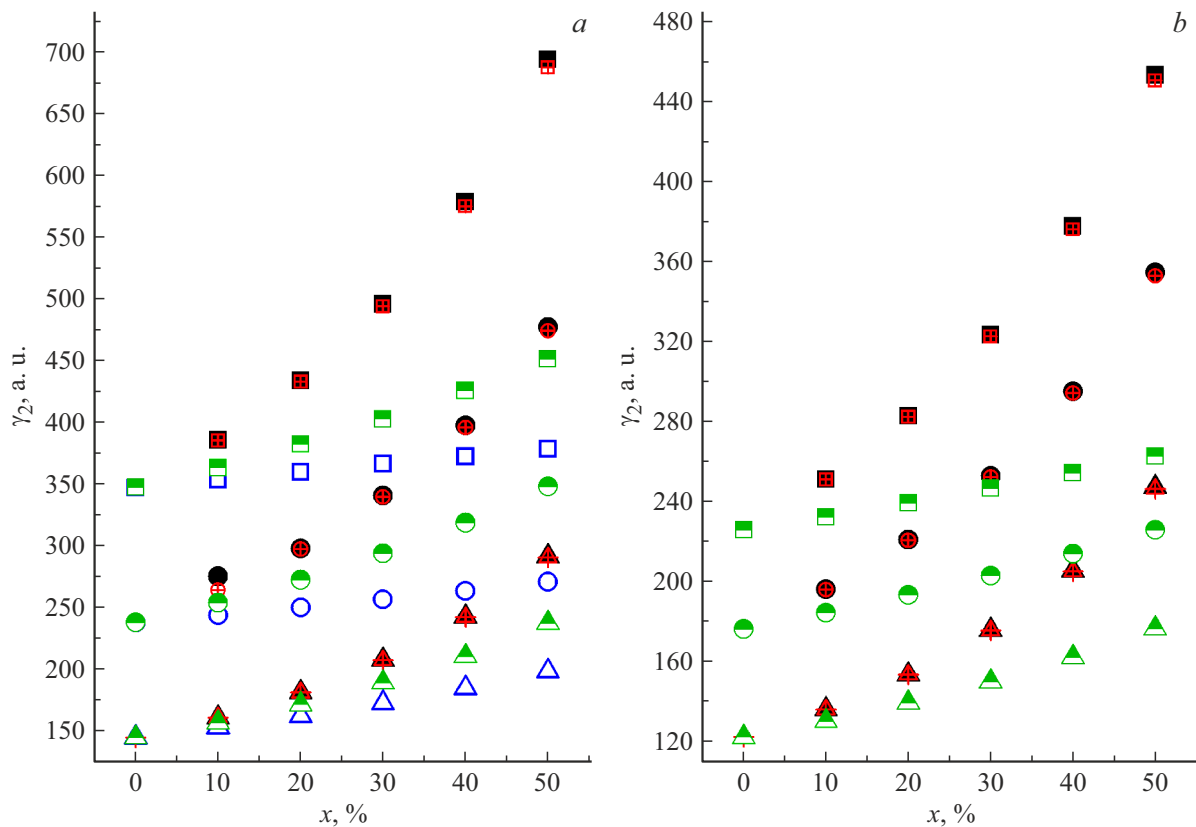


**Figure 2.** Change in the kurtosis coefficient ( $\gamma_2$ ) of the Bragg reflection with an increase in the percentage of the bulk material phase in the sample ( $x$ ) in the case of various combinations of nanophase and bulk line shapes: the nanostructured phase is described by the pseudo-Voigtian (*a*), Lorentzian (*b*); the bulk one — by Gaussian (black filled symbols), squared Lorentzian (red crossed symbols (online)), Lorentzian (blue empty symbols (online)). The half-filled green symbols (in the online version) in both cases correspond to the case of the same line shape. Squares correspond to particle size 80 nm, circles — 40 nm, triangles — 20 nm.

resolution and the broadening of the elastic peak due to the size effect using the Debye–Scherrer formula:

$$H_{size} = \frac{k\lambda}{d \cos \theta}, \quad (6)$$

in which the coefficient  $k$  was set equal to one,  $d$  — the average diffraction size of nanoparticles,  $2\theta$  — the position of the Bragg reflection.

The summation of the contributions of instrumental and dimensional broadening was carried out according to the following formulas:

— in the case of a Gaussian

$$H_G^2 = H_{instr}^2 + H_{size}^2, \quad (7)$$

— for Lorentzian and squared Lorentzian

$$H_L = H_{instr} + H_{size}, \quad (8)$$

— in case of pseudo-Voigtian [11]:

$$H_{pV}^5 = H_G^5 + 2.69269H_G^4H_L + 2.42843H_G^3H_L^2 + 4.47163H_G^2H_L^3 + 0.07842H_GH_L^4 + H_L^5, \quad (9)$$

$$\eta = 1.36603 \frac{H_L}{H_{pV}} - 0.47719 \left( \frac{H_L}{H_{pV}} \right)^2 + 0.11116 \left( \frac{H_L}{H_{pV}} \right)^3. \quad (10)$$

The variance  $\sigma$ , the asymmetry coefficient  $\gamma_1$ , and the kurtosis  $\gamma_2$  were calculated in terms of the central moments 2, 3, and 4 orders of  $\mu_2, \mu_3, \mu_4$  using the formulas [9]:

$$\sigma = \sqrt{\mu_2},$$

$$\gamma_1 = \frac{\mu_3}{\sigma^3},$$

$$\gamma_2 = \frac{\mu_4}{\sigma^4} - 3.$$

## 2. Results of modelling and discussion

Figures 1–3 show the results of calculations of the dependences of parameters  $\sigma$  (Fig. 1),  $\gamma_2$  (Fig. 2) and  $\gamma_1$  (Fig. 3) on percentage content of impurity phase of bulk material  $x$ . Fig. 1, *a*–3, *a* correspond to the variant when the nanostructured phase is described by a pseudo-Voigtian, and the bulk — by various types of profiles (Gaussian, Lorentzian, squared Lorentzian, and also for comparison added dependencies for the pseudo-Voigtian

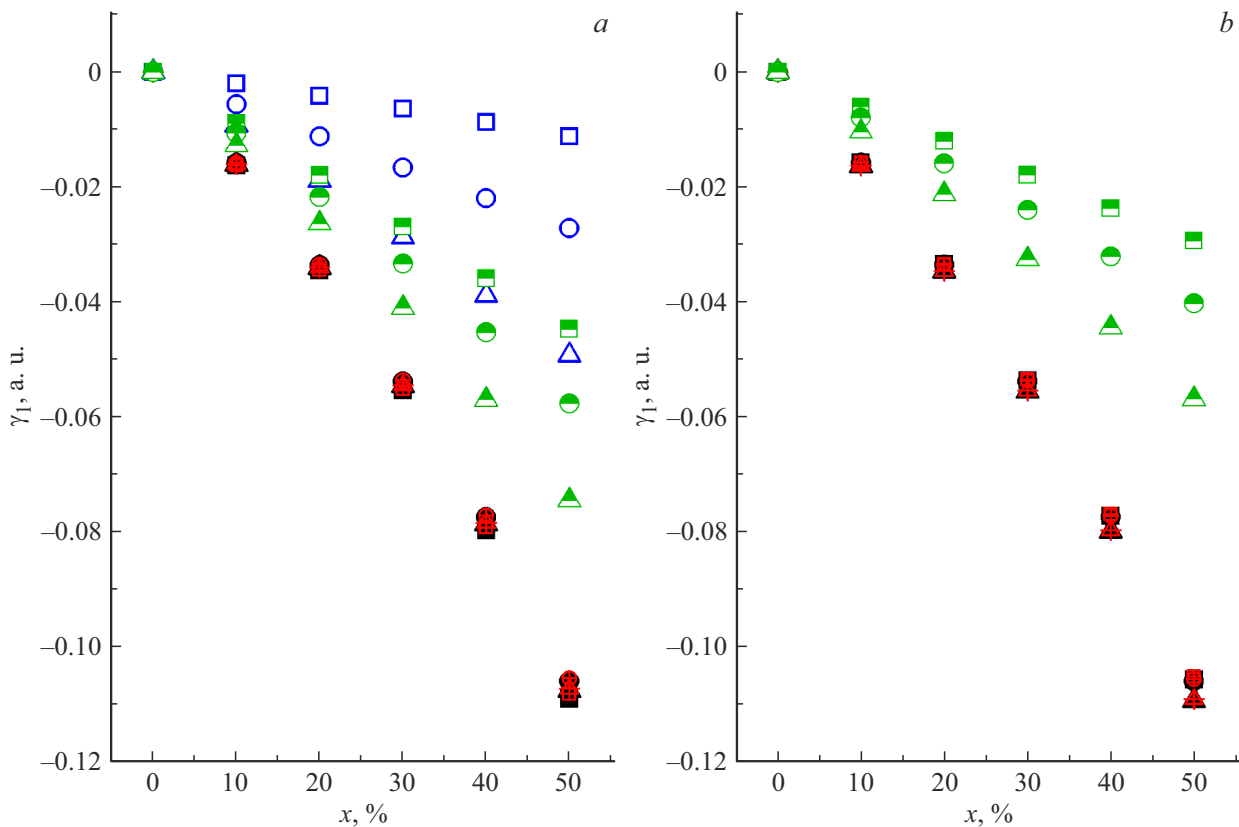


**Figure 3.** Change in the asymmetry coefficient ( $\gamma_1$ ) of the Bragg reflection with an increase in the percentage of the bulk material phase in the sample ( $x$ ) in the case of various combinations of nanophase and bulk line shapes: the nanostructured phase is described by the pseudo-Voigtian (*a*), Lorentzian (*b*); the bulk one — by Gaussian (black filled symbols), squared Lorentzian (red crossed symbols (in online version)), Lorentzian (blue empty symbols (in online version)). The half-filled green symbols (in the online version) in both cases correspond to the case of the same line shape. Squares correspond to particle size 80 nm, circles — 40 nm, triangles — 20 nm.

from the article [8]). In Fig. 1, *b*–3, *b* the response from nanoparticles is described by the Lorentzian, and the bulk fraction is described by the Gaussian, squared Lorentzian and Lorentzian. In all figures, the calculation error does not exceed the symbol size. As in the work [8], the dependences are calculated for the cases when the cell parameters of the nanostructured and bulk phases coincide and for the case when they differ, but since the dependences of the variance and kurtosis coefficient on the difference between the cell parameters in all considered cases is not found and the results coincide within the error bars, then, in order to avoid the overloading of the figures, the results for the case of different cell parameters are not shown.

From these dependencies, the following conclusions can be drawn:

- with an increase in the percentage of bulk material, the dispersion decreases;
- the kurtosis coefficient increases with an increase in the content of the bulk fraction;
- in the case of different cell parameters of the nanostructured and bulk phases, the value of the asymmetry coefficient  $\gamma_1$  increases in absolute value with the increasing content of the bulk phase.

Thus, all regularities noted in the paper [8] for the case of identical functions (Gaussian, Lorentzian, pseudo-Voigtian) of contributions from bulk and nanostructured materials are also observed for cases when these functions differ. At the same time, some features should be noted, in particular, if the functions describing the contributions from the array and nanoparticles differ greatly in the decay rate of the „tails“ (for example, in the case of a combination when the bulk is described by a Gaussian or a squared Lorentzian, and nanostructured phase — by pseudo-Voigtian or Lorentzian), then the difference between the values of  $\sigma$ ,  $\gamma_1$ , and  $\gamma_2$  at different concentrations of the bulk fraction becomes much larger than for the case of identical line profiles. Note that, in this case, the dependence of the asymmetry coefficient on the diffraction size of the particles vanishes. Thus, the proposed method makes it possible to isolate the contribution of the bulk material impurity even more reliably.

For the case when the bulk is described by the Lorentzian and the nanostructured phase by the pseudo-Voigtian, the opposite situation is observed: the difference between the values of the line distortion parameters at different values of  $x$  becomes somewhat smaller than in the case of the same

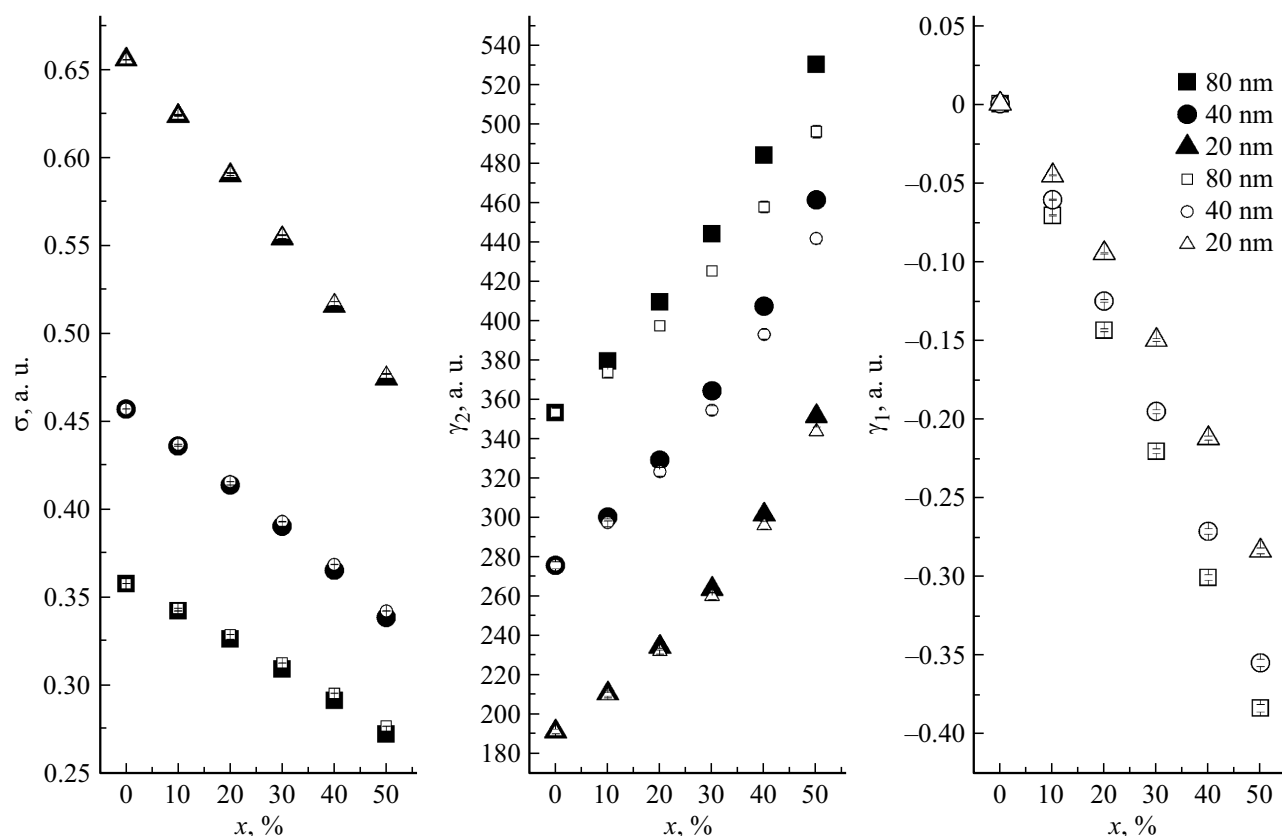


**Figure 4.** Dependences of the parameters  $\sigma$ ,  $\gamma_1$  and  $\gamma_2$  on the percentage of the bulk material phase in the sample ( $x$ ) in the case of a combination of line profiles bulk–Gaussian, nanophase–squared Lorentzian at different particle sizes and different ratios of the lattice parameters of the array and the nanostructured phase (black symbols — lattice parameters are the same, empty symbols — lattice parameters of the array and nanophase are different).

line shape, but still allows apply the developed algorithm. For a combination of profile functions that are similar in tail decay (for example, bulk is described by a Gaussian, and a nanophase by a squared Lorentzian), all regularities are observed that are typical for the case of a Gaussian shape of the bulk line and nanophase considered in the previous work. The dependences of the parameters  $\sigma$ ,  $\gamma_1$ , and  $\gamma_2$  are shown in Fig. 4.

### 3. Stability of the algorithm to level background

A real experimental diffraction pattern always contains a certain background, and the „signal–background“ ratio affects the accuracy of determining the parameters that describe the shape of the signal line. In this section, we consider the influence of this ratio on the value of the error in determining the variance  $\sigma$  for the two most unfavorable cases. In both cases, the nanostructured phase is described by the Gaussian, while the impurity of the bulk fraction is 10% and is described either by the Voigtian (*a*) or by the squared Lorentzian (*b*). In both cases, the size of nanoparticles in the simulation was 80 nm (i.e., the broadening due to the size effect is small), and the unit

cell parameters are the same. The model spectra were modulated with „white noise“: an example of the resulting spectrum is shown in Fig. 5.

The amplitude ratio „signal–noise“ varied from 0 to 60%. The results of the above simulation (values for the variance  $\sigma$  of the elastic peak) are shown in Fig. 6, *a* for the combination of Gaussian+Voigtian functions and in Fig. 6, *b* for a pair of Gaussian+squared Lorentzian. Black squares correspond to the case of the absence of an admixture of bulk material, and red circles (in the online version) — NCM, in which there is 10% of the bulk phase. The given errors correspond to a confidence interval of three standard deviations.

From Fig. 6 it is clearly seen that with the addition of noise, not only the values of the dispersion parameters  $\sigma$  for the elastic peak increase, but also the corridors of three standard errors of these parameters. In the case when these intervals for the values  $\sigma$  at  $x = 0$  and 10% overlap, we can say that using this method it is impossible to reliably detect the presence of an admixture of bulk material equal to 10%. It is easy to see that for a combination of profile functions Gaussian + Voigtian this threshold corresponds to a noise level of about 60%, and for a combination of Gaussian + squared Lorentzian it is slightly less than 50%.

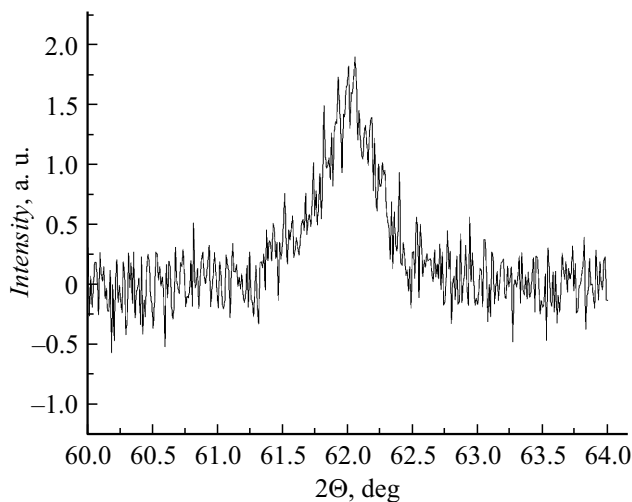


**Figure 5.** An example of a signal from an elastic peak described by a combination of Gaussian and Voigtian and modulated „by white noise“. Amplitude ratio noise — signal is 60%.

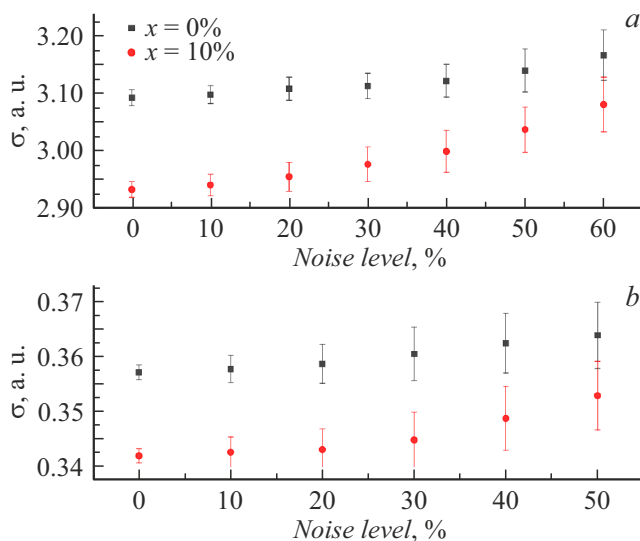


**Figure 6.** Dependences of  $\sigma$  dispersion values with increasing noise level for cases of pure nanostructured phase ( $x = 0\%$ ) and for NCM, in which 10% impurities of bulk fraction ( $x = 10\%$ ), for different combinations of the profile functions of the bulk and the nanostructured phase: *a* — Gaussian+Voigtian, *b* — Gaussian+squared Lorentzian.

Thus, it is shown that the proposed method works even with a rather poor noise/signal ratio.

## Conclusion

The influence of the bulk phase impurity on the distortion of the line shape of elastic peaks for nanocomposite materials based on porous nanomatrices is analyzed for the main functions describing the diffraction peaks of nanocomposite materials, taking into account the instrumental resolution

function. It is shown that the use of higher central moments of the distribution makes it possible to determine the contribution of the bulk fraction with an accuracy of 5–10%, and the proposed algorithm does not require a full-scale profile analysis. This algorithm works well even with a poor noise/signal ratio: it is shown that the stability is preserved even in the case when the noise/signal ratio reaches 60%.

## Funding

O.A. Alekseeva is grateful to the RFBR-BRICS grant №19-52-80019 for partial financial support for the work on this topic.

## Conflict of interest

The authors declare that they have no conflict of interest.

## References

- [1] C.T. Kresge, M.E. Leonowicz, W.J. Roth, J.C. Vartuli, J.S. Beck. *Lett. Nature*, **359**, 710 (1992). DOI: 10.1038/359710a0
- [2] M. Grün, I. Lauer, K. Unger. *Adv. Mater.*, **9**, 254 (1997). DOI: 10.1002/adma.19970090317
- [3] W. Zhao, Q. Li. *Chem. Mater.*, **15**, 4160 (2003). DOI: 10.1021/cm034570k
- [4] Yu. Kumzerov, S. Vakhrushev. *Encyclopedia of Nanoscience and Nanotechnology*, ed. H.S. Nalwa (American Scientific Publishers, 2004), v. VII, p. 811.
- [5] V.N. Bogomolov, D.A. Kurdyukov, L.S. Parfen'eva, A.V. Prokof'ev, S.M. Samoilovich, I.A. Smirnov, A. Jezowski, J. Mucha, H. Misiorek. *Phys. Solid State*, **39** (2), 341 (1997). DOI: 10.1134/1.1129776
- [6] I.V. Golosovsky, O.P. Smirnov, R.G. Delaplane, A. Wannberg, Y.A. Kibalin, A.A. Naberezhnov, S.B. Vakhrushev. *Eur. Phys. J.*, **B54**, 211 (2006). DOI: 10.1140/epjb/e2006-00446-8
- [7] A.A. Naberezhnov, S.A. Borisov, A.V. Fokin, A.Kh. Islamov, A.I. Kuklin, Yu.A. Kumzerov. *Nanosystems: Phys., Chem., Mathem.*, **11** (6), 690 (2020). DOI: 10.17586/2220-8054-2020-11-6-690-697
- [8] O.A. Alekseeva, A.A. Naberezhnov. *ZhTF*, **92** (1), 155 (2022). DOI: 10.21883/JTF.2022.01.51866.208-21
- [9] G. Kramer. *Mathematical Methods of Statistics* (Mir, M., 1975)
- [10] G. Caglioti, A. Paoletti, F.P. Ricci. *Nucl. Instrum.*, **3**, 223 (1958). DOI: 10.1016/0369-643X(58)90029-X
- [11] P. Thompson, D.E. Cox, J.B. Hastings. *J. Appl. Cryst.*, **20**, 79 (1987). DOI: 10.1107/S0021889887087090